

---

Position-sensitive detectors for gamma ray imaging

Peter Dendooven<sup>1</sup>  
Santeri Saariokari<sup>1</sup>  
Peter Andersson<sup>2</sup>  
Sofia Godø<sup>3</sup>  
Anders Puranen<sup>4</sup>  
Gustav Pettersson<sup>4</sup>  
Stefan Jarl Holm<sup>2</sup>  
Erik Brücken<sup>1</sup>  
Mihaela Bezak<sup>1</sup>  
Matti Kalliokoski<sup>1</sup>  
Vikram Rathore<sup>2</sup>  
Mounia Laassiri<sup>5</sup>  
Ramsey Al Jebali<sup>3</sup>  
Aage Kalsæg<sup>3</sup>

<sup>1</sup>Helsinki Institute of Physics, University of Helsinki, Helsinki, Finland

<sup>2</sup>Department of Physics and Astronomy, Uppsala University, Uppsala, Sweden

<sup>3</sup>Integrated Detector Electronics AS (IDEAS), Oslo, Norway

<sup>4</sup>AB Svafo, Nyköping, Sweden

<sup>5</sup>Department of Physics, Brookhaven National Laboratory, Upton, NY, USA

## **Abstract**

The POSEIDON project activities between March 2024 and February 2025 are summarized. Monte Carlo simulations show the clear advantage of large CZT detectors compared to the presently used small detectors for PGET of spent nuclear fuel was demonstrated: the efficiency to detect the full energy of the gamma rays from the decay of  $^{137}\text{Cs}$  is more than 20 times larger. This justifies the further development of the large CZT detectors. The results of a first measurement campaign combining a tomographic setup at Uppsala University with a detector from IDEAS in Oslo and a collimator from HIP in Helsinki demonstrates the feasibility of PGET measurements using state-of-the-art large position-sensitive CZT detectors, showing that such detectors are a viable choice for future development of the PGET method. This experimental work is being complemented with Monte Carlo simulation of PGET of real spent nuclear fuel. First results, using a somewhat simplified gamma ray emission source, demonstrate that the Monte Carlo framework performs well. A measurement campaign using two commercial gamma ray imagers, the CZT-based H420 and the germanium-based GeGI, in a realistic nuclear waste setup at Svafo and a real-life decommissioning situation at TSL, has resulted in valuable practical experience with both imagers. The conclusion is that both imagers perform similarly, with the H420 being somewhat easier to handle and operate. The activities have increased knowledge and expertise in the Northern Countries on several topics related to gamma ray imaging. A brief outlook of the continuing activities over the next year is presented.

## **Key words**

gamma ray imaging, position sensitive detectors, semiconductor detectors, spent nuclear fuel, decommissioning, nuclear waste, tomography



# **Position-sensitive detectors for nuclear fuel imaging (POSEIDON)**

## **Final Report from the NKS-R POSEIDON activity (Project: NKS-R-2022-136)**

Peter Dendooven<sup>1</sup>  
Santeri Saariokari<sup>1</sup>  
Peter Andersson<sup>2</sup>  
Sofia Godø<sup>3</sup>  
Anders Puranen<sup>4</sup>  
Gustav Pettersson<sup>4</sup>  
Stefan Jarl Holm<sup>2</sup>

Erik Brücken<sup>1</sup>  
Mihaela Bezak<sup>1</sup>  
Matti Kalliokoski<sup>1</sup>  
Vikram Rathore<sup>2</sup>  
Mounia Laassiri<sup>5</sup>  
Ramsey Al Jebali<sup>3</sup>  
Aage Kalsæg<sup>3</sup>

<sup>1</sup>Helsinki Institute of Physics, University of Helsinki, Helsinki, Finland

<sup>2</sup>Department of Physics and Astronomy, Uppsala University, Uppsala, Sweden

<sup>3</sup>Integrated Detector Electronics AS (IDEAS), Oslo, Norway

<sup>4</sup>AB Svafo, Nyköping, Sweden

<sup>5</sup>Department of Physics, Brookhaven National Laboratory, Upton, NY, USA



## Table of contents

	Page
1. Introduction	3
2. Monte Carlo simulations of PGET with small and large CZT detectors	4
2.1. The MC simulation framework	4
2.2. Response of small and large CZT detectors	4
2.3. Tomography	6
3. Tomographic measurements with a large CZT detector	7
3.1. Setup and measurement procedure	7
3.2. Results	8
4. Gamma ray imagers for waste characterization and decommissioning	10
4.1 The H420 and GeGI gamma ray imagers	10
4.2. Measurement environments	10
4.3. Results	11
5. Conclusions	13
6. References	14

## 1. Introduction

The results of the first year of the POSEIDON project NKS-R-2022-136, which ran from June 2022 to May 2023, are presented in the NKS-473 report (Laassiri et al., 2023). This document reports the outcome of the continuation and broadening of the POSEIDON project between March 2024 and February 2025.

In the POSEIDON project, various developments of 3D position-sensitive semiconductor detectors for gamma ray imaging are being pursued. The focus is on applying state-of-the-art Cadmium Zinc Telluride (CZT) detectors for passive gamma emission tomography (PGET) of spent nuclear fuel assemblies (SFA), and both CZT-based and germanium-based imaging devices for the decommissioning of nuclear sites and the characterization of legacy waste.

Regarding spent nuclear fuel imaging, we investigate further development of the PGET device for imaging SFAs which was developed under the guidance of IAEA and approved for nuclear fuel inspections by IAEA in 2017. The PGET device is based on a collimator consisting of a linear array of narrow slits, with a small CZT detector behind each slit (Mayorov et al., 2017, Virta et al., 2022). Because of the small detectors, the probability that a gamma ray is fully absorbed, providing ideal imaging information, is small. Large CZT detectors would have a higher probability for detecting the full energy of gamma rays, increasing the sensitivity and image quality of the PGET device. However, a large CZT detector would cover more than one collimator slit, requiring position sensitivity to determine through which slit a gamma ray travelled in order to maintain image spatial resolution. Additionally, Compton imaging can provide information on the axial distribution of the SFA activity. Section 2 describes the extension of the simulation framework to full tomographic procedures. Part of the results have been recently published (Saariokari 2025). Section 3 reports on the measurements with a large state-of-the-art CZT detector combined with a PGET slit collimator and  $^{137}\text{Cs}$  rod-shaped radioactive sources.

Many countries need to take care of facilities and waste from early nuclear research programs in a safe and environmentally responsible manner. In Sweden, AB Svafo is a not-for-profit company owned by the Swedish nuclear power plants dedicated to this task. Activities include decommissioning of the Studsvik R2 reactor and modernization of facilities in Studsvik for safe interim storage of radioactive materials. A major undertaking is long term management, handling, sorting and conditioning of legacy nuclear waste for either free-release, recycling or disposal. The POSEIDON project plays a role in the evaluation and R&D of non-destructive test methods as well as novel waste handling techniques, which are of high priority during the coming years in preparation of more industrial scale waste handling, classification and conditioning for disposal later in the century. In section 4, the results of comparing a CZT-based and a germanium-based commercial gamma imaging device in decommissioning and legacy waste environments, are described.

## 2. Monte Carlo simulations of PGET with small and large CZT detectors

### 2.1 The MC simulation framework

Figure 1 shows the geometry of the source, slit collimator and CZT detectors implemented using the GEANT4 framework (Allison et al., 2016). A small CZT detector is placed behind each slit, whereas each large CZT detector covers 5 slits. A rod-shaped radioactive source emitting either 662 keV or 1274 keV primary gamma rays was defined. These gamma ray energies are characteristic of the decay of  $^{137}\text{Cs}$  and  $^{154}\text{Eu}$ , the main gamma ray emitting fission products in spent nuclear fuel after a cooling time of a few years.

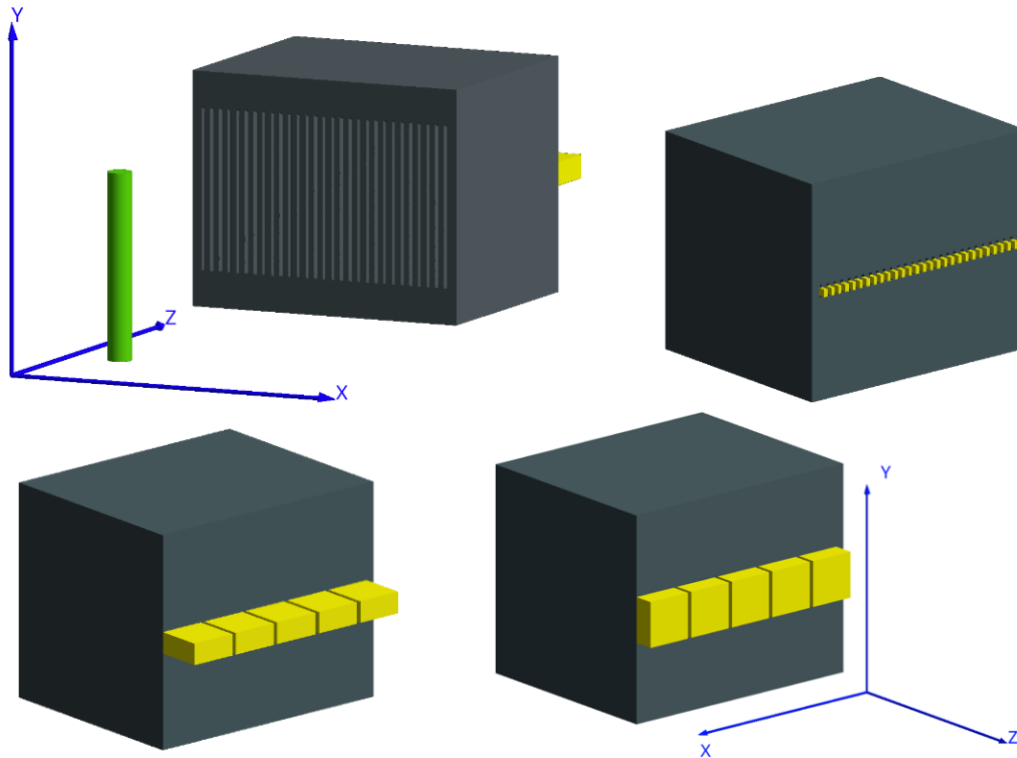


**Figure 1.** Implementation of radioactive source (green), slit collimator (gray) and CZT detectors (yellow) in the GEANT4 framework. The 100 mm thick tungsten collimator contains 1.5 mm wide slits with a pitch of 4 mm. The slits are conical, with a height 70 mm at the front and 5 mm at the back of the collimator. Top right: a small CZT detector ( $1.75 \times 3.5 \times 3.5 \text{ mm}^3$ ) is placed behind each slit. The large CZT detectors are placed in two orientations:  $22 \times 10 \times 22 \text{ mm}^3$  (bottom left, orientation 1) and  $22 \times 22 \times 10 \text{ mm}^3$  (bottom right, orientation 2).

### 2.2 Response of small and large CZT detectors

Energy spectra are created as histograms of the energy deposited in a detector per primary gamma ray event. Figure 2 shows the energy spectra for both gamma ray energies and the three detector configurations. The usual main features of gamma ray energy spectra are observed: full-energy peak, Cd, Zn and Te X-ray escape peaks at about 25 keV below the full-energy peak and Compton edge at 478 keV, resp. 1061 keV, for the 662 keV, resp. 1274 keV primary gamma ray energies. As the 1274 keV gamma ray can interact via pair production, its spectrum shows very weakly the single and double positron annihilation photon escape peaks (at 764 and 253 keV), as well as a 511 keV peak related to positron annihilation outside of the detector. The tungsten characteristic X-rays at 58 and 67 keV created in the collimator are visible as well. Overall, the spectrum intensity is much higher for the large than for the small CZT detectors and there is a minor difference in intensity between the two orientations of the large detectors. Table 1 compares the full-energy peak intensities, showing the large gain in sensitivity of the large detectors.

The position-sensitive detectors can be used for Compton imaging as, in principle, the different interaction locations of a primary gamma ray can be distinguished. The "golden" events for Compton imaging are those in which Compton scattering is followed by photoelectric effect, resulting in the full absorption of the primary gamma ray energy. Table 1 shows the fraction of such golden events relative to the total number of interactions for both large crystal orientations and primary gamma ray energies. As far as Compton imaging is concerned, there is no significant difference between the two detector orientations.

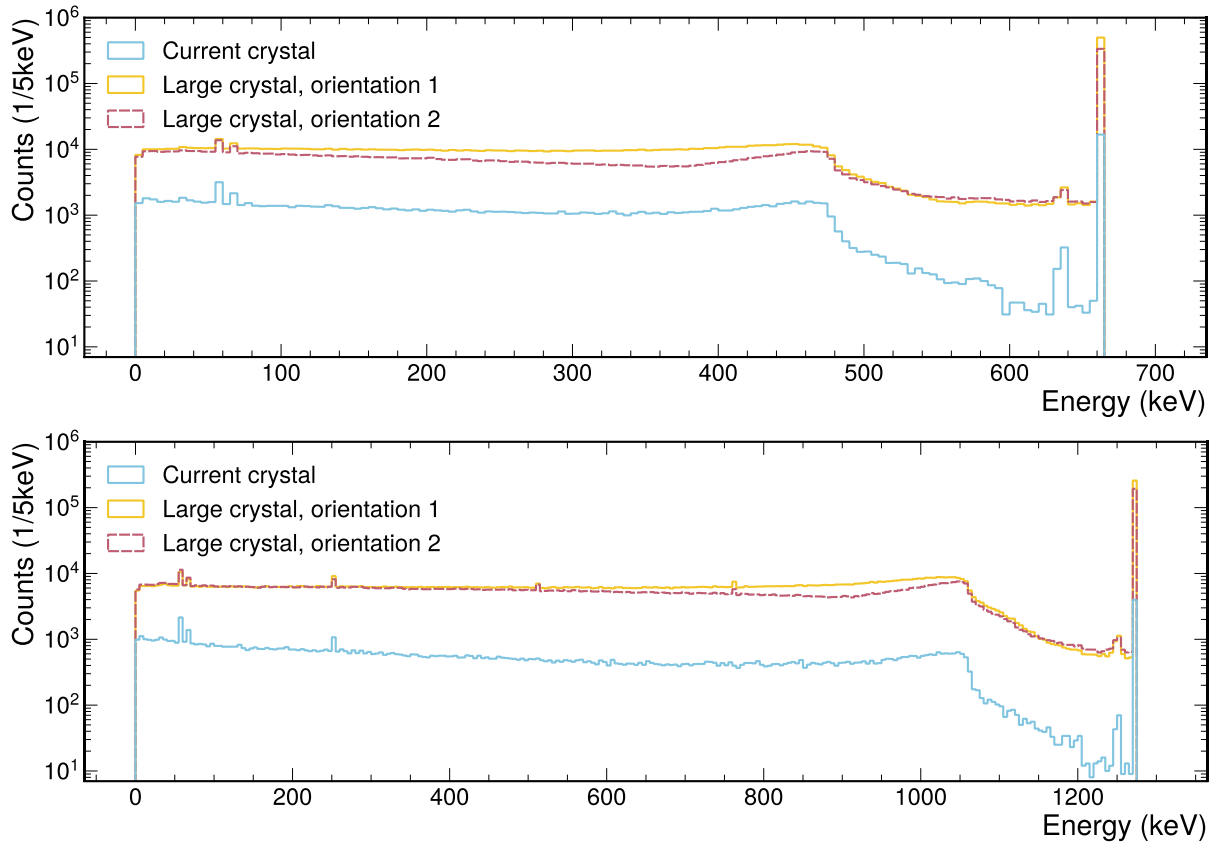


**Figure 2.** Energy spectra of the small CZT detectors (Current crystal) and the two orientations of the large CZT detectors (Large crystal), for 662 keV (top) and 1274 keV (bottom) primary gamma ray energies.

**Table 1.** Full-energy peak intensities (normalised to the small CZT detectors) and fraction of golden events for Compton imaging relative to the total number of interactions. Values for both large detector orientations and primary gamma ray energies are given.

CZT detector	full-energy peak intensity		fraction of golden events (%)	
	662 keV	1274 keV	662 keV	1274 keV
small	1	1	–	–
large, orientation 1	29	65	13.6	7.4
large, orientation 2	20	48	14.0	7.6

## 2.3 Tomography

Full PGET tomographic simulations were performed for the large CZT detectors in orientation 1. Figure 3, top, shows the simulation geometry and some gamma ray paths. In this preliminary simulation, all gamma rays are emitted in the central plane of the tomograph. A VVER-440 fuel assembly with three missing fuel rods (not shown in Figure 3), emitting either 662 keV or 1274 keV gamma rays, was considered. Tomographic data is simulated by rotating the fuel assembly over 360 degrees in 1-degree steps. The resulting sinogram is shown in Figure 3, bottom.

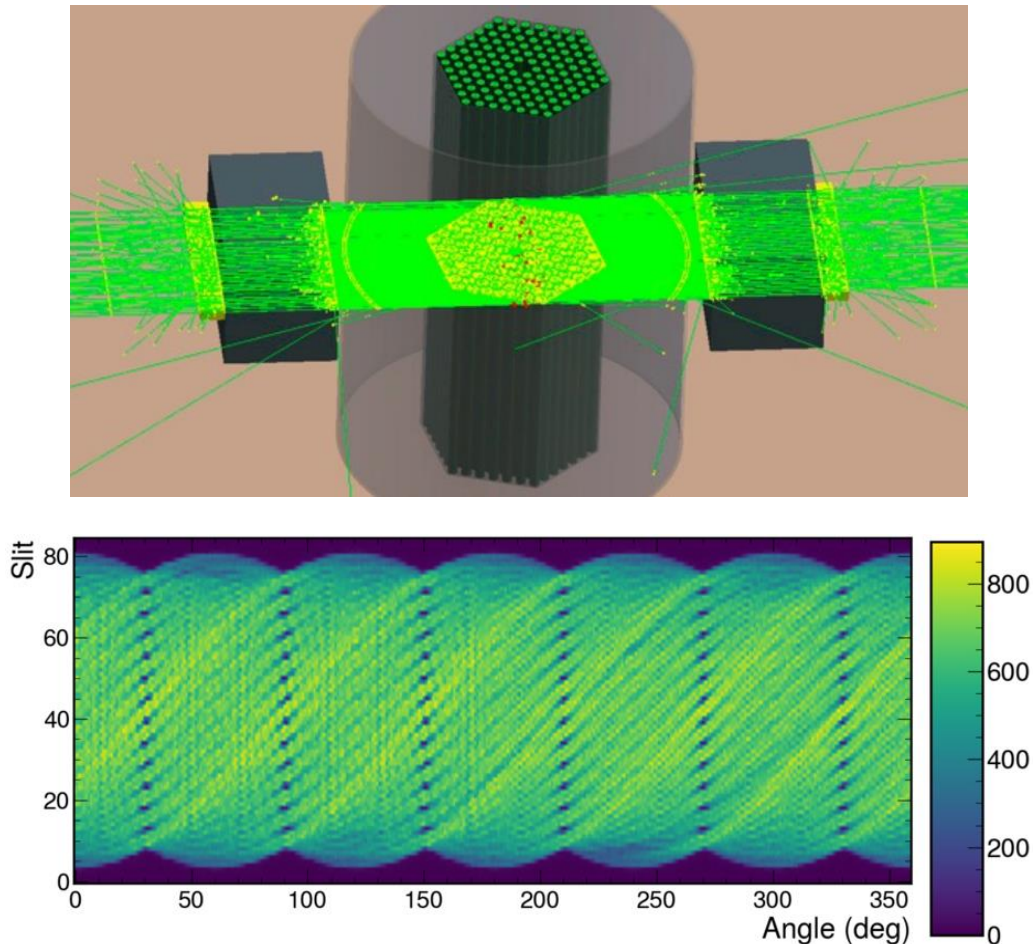


**Figure 3.** Top: geometry of the GEANT4 PGET tomographic simulations considering the large CZT detectors in orientation 1. The PGET device has two detector banks, on opposite sides of the fuel assembly. Some gamma ray paths are shown in green. Bottom: Sinogram obtained after combining the counts from the two detector banks.

Presently, more realistic simulations are being prepared to be run on a high-performance computer cluster. These will consider a homogeneous distribution of the gamma-emitting nuclides throughout the length of the fuel rods and isotropic emission of gamma rays. The resulting sinograms will be used for image reconstruction using the iterative reconstruction method previously developed in a collaboration of the University of Helsinki and STUK (Backholm et al., 2020, Virta et al., 2020) and being used in the PGET safeguards inspections at the Finnish geological repository for spent nuclear fuel.



### 3. Tomographic measurements with a large CZT detector

#### 3.1 Setup and measurement procedure

An experimental setup was assembled at Uppsala University, containing the following items (see Figure 4):

- the refurbished Bettan tomographic setup (Jansson et al., 2013) with rod-shaped  $^{137}\text{Cs}$  sources, available at Uppsala University;
- a large CZT detector: an IDEAS GDS-100 system containing two  $22\times 22\times 10\text{ mm}^3$  CZT detectors, contributed by Integrated Detector Electronics AS (IDEAS);
- a 1D multi-slit tungsten collimator identical to the one in the PGET device, contributed by the Helsinki Institute of Physics (HIP).

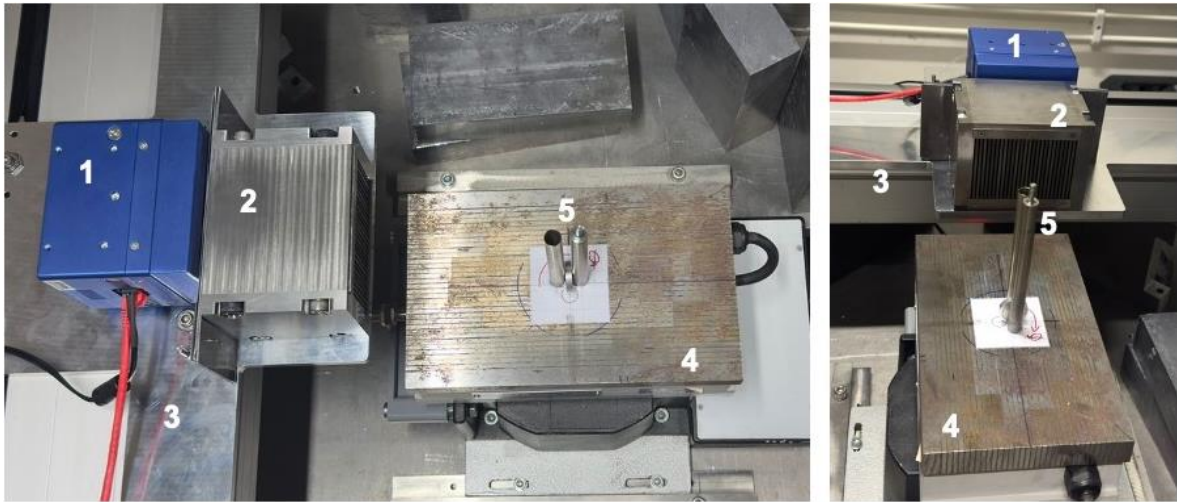


**Figure 4.** Tomographic setup at Uppsala University. 1: GDS-100 CZT detector; 2: PGET-type collimator; 3: lateral translation stage; 4: rotation stage; 5:  $^{137}\text{Cs}$  radioactive sources (note that one of the rods in these photographs is an empty container, which was replaced by a  $^{137}\text{Cs}$  source for the tomography measurements).

Two rod-shaped sources were placed with 5 mm spacing. The combination of 4 lateral translational steps of the detector/collimator (see Figure 5, left) with 120 angular 3-degree steps of the rotation stage resulted in 480 individual measurements for each of the two CZT detectors.

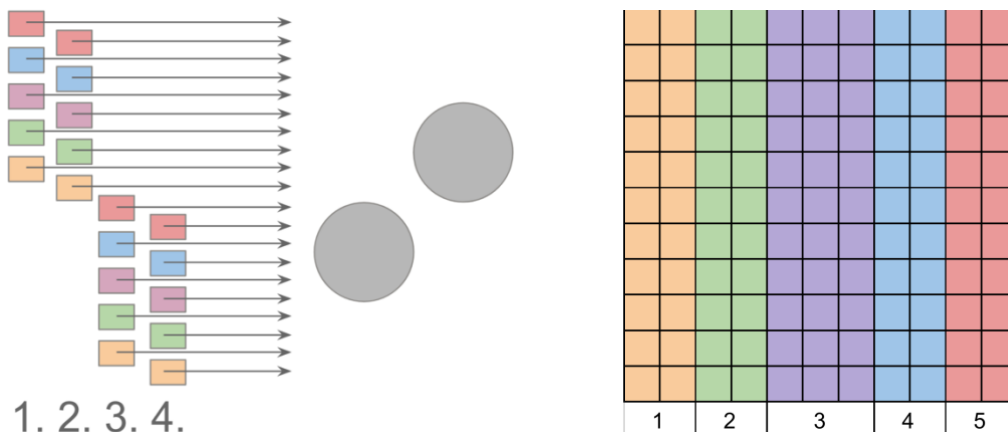


**Figure 5.** Left: Four lateral positioning steps (numbered 1 to 4) of the detector-collimator system during a single angular step of the tomographic scan. Groups of detector pixels corresponding to a collimator slit are visualised as a colored rectangle. The radioactive rods are shown in gray. A single CZT detector covers 5 collimator slits. The drawing is not to scale. Right: grouping of detector pixels used to extract information per collimator slit, numbered from 1 to 5. Pixels with the same color have their data combined.

The full scan sequence was performed for the two different CZT crystals with identical nominal performance positioned in the ASIC 2 and 3 neighboring slots of the GDS-100. The intensity per slit was determined by combining the data from pixels covering the corresponding slit, as illustrated in Figure 5, right.

The measured detector signals were post-processed to contain only pulses related to the photo peak by discarding pulses smaller than a set threshold. A sinogram is created by combining the four “sub steps” of each angular step into one projection and combining the projections from all rotational steps into a full sinogram. Finally, an image reconstruction is performed using a simple filtered backprojection algorithm to verify the correctness of the measurement.

### 3.2 Results

Figure 6 shows the amplitude spectrum over all pixels. An amplitude threshold of 700 was chosen to select only the  $^{137}\text{Cs}$  full-energy peak to be used in the sinogram.

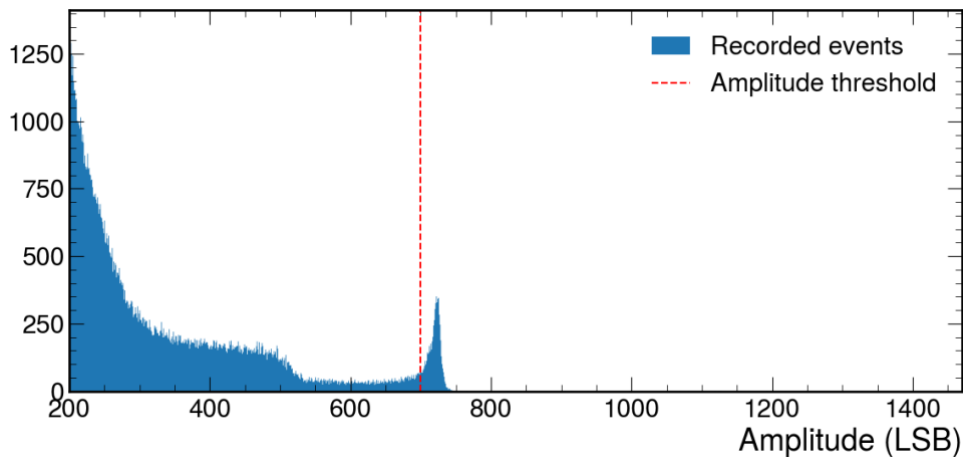


**Figure 6.** Amplitude spectrum over all pixels. The vertical dashed line represents the amplitude threshold.

A light Gaussian smoothing filter was applied to the sinogram to remove occasional dark spots, presumably caused by operational effects of the detector. A total of 6 measurements out of 960 were found to be defective with partially or fully missing data.

Figure 7 presents the main results for the detector in the ASIC 3 position. Processing of the individual measurements resulted in a sinogram covering the radioactive sources with a linear step of 2 mm and a full rotation with an angular step of 3 degrees. The reconstructed 2D image shows a clear picture of the two rod-shaped radioactive sources. The image line profile through the center of the rods shows an activity ratio of the two rods of 2.20 with ASIC 2 and 2.11 with ASIC 3. This is within the factor 2.3 range of variation amongst the 70 rod sources available (Jansson et al., 2013). The results demonstrate excellent imaging quality when using large position-sensitive CZT detector for spent fuel imaging in a PGET-like device.

This proof of principle of the use of pixelated CZT detectors with a PGET type collimator for tomography demonstrates that pixelated detectors are a viable choice for future development of the PGET method.

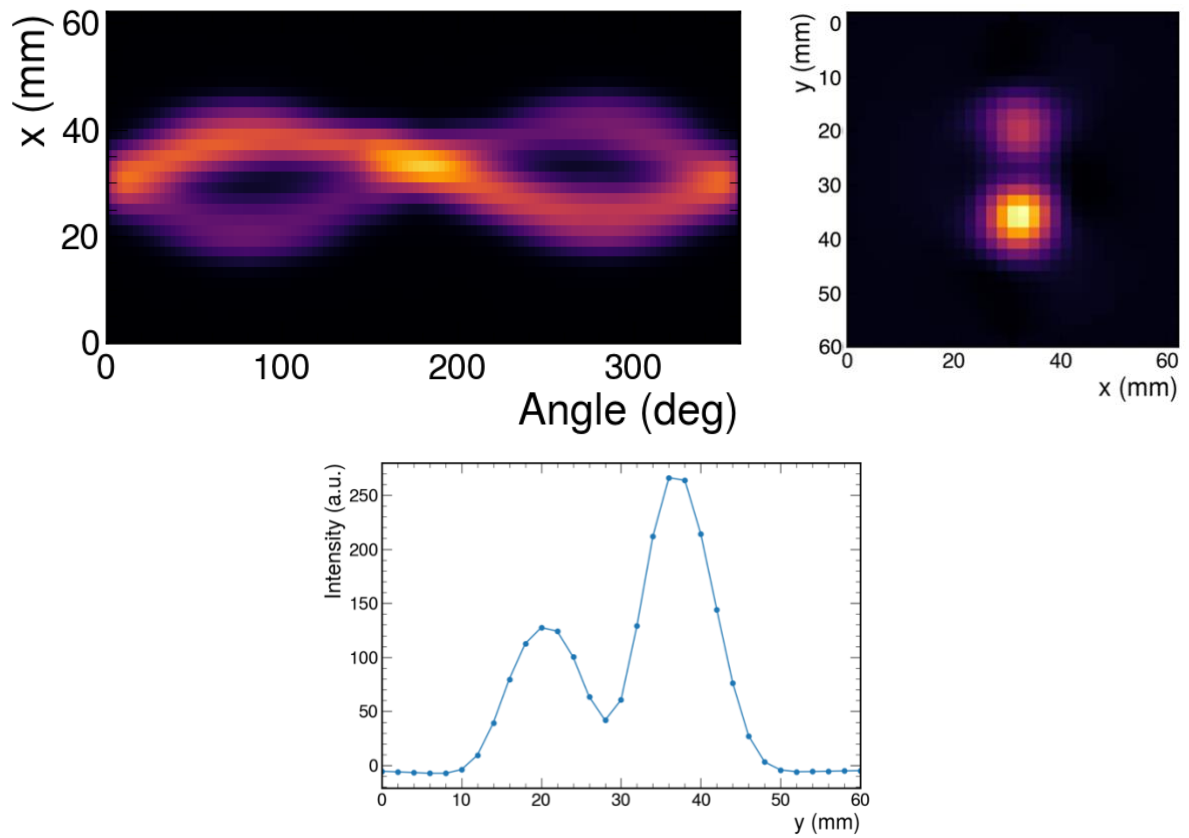


**Figure 7.** Top left: sinogram of the tomographic measurement of two rod-shaped  $^{137}\text{Cs}$  sources using a GDS-100 large CZT detector and a PGET-type 1D multi-slit collimator. Top right: 2D image reconstructed from the sinogram on the left. Bottom: image vertical line profile through the center of the rods.

## 4. Gamma ray imagers for waste characterization and decommissioning

### 4.1 The H420 and GeGI gamma ray imagers

The H420 and GeGI gamma ray imaging spectrometers are commercial gamma ray cameras based on position-sensitive semiconductor detectors. Table 2 gives some basic information on these devices. The measurements performed compared the H420 device owned by Svafo with the GeGI device owned by HIP. Both devices can operate in Compton imaging mode. For low gamma-ray energies, the H420 operates in coded-aperture mode, whereas the GeGI operates with a pinhole collimator. Newer versions of the GeGI also have a coded aperture add-on option.

**Table 2.** Comparison of the basic properties of the H420 and GeGI gamma ray imagers.

	H420	GeGI
manufacturer	H3D Inc.	PHDS Co.
detector crystal properties:		
material	CZT	germanium
size	4 crystals of 22×22×10 mm <sup>3</sup> >19 cm <sup>3</sup> active volume	90 mm diameter, 11 mm thick 67 cm <sup>3</sup> active volume
pixellated readout	11×11 pixels anode, 1 cathode	16 anode strips, 16 cathode strips (orthogonal), 5 mm pitch
energy resolution (FWHM at 662 keV)	≤ 1.1% (≤ 7.3 keV)	< 0.3% (< 2.1 keV)
spatial resolution (FWHM)	0.5 mm in 3D	1.5 mm in 3D
device dimensions	24 cm × 9.5 cm × 18 cm	26 cm × 20 cm × 14 cm
device weight	3.6 kg	6.8 kg

### 4.2 Measurement environments

Measurements were performed in a shielded chamber at Svafo and at the The Svedberg Laboratory (TSL), the particle accelerator facility at Uppsala University that was shut down in 2016 and whose decommissioning is planned to be completed in 2026.

The setup at Svafo is shown in Figure 8. Next to the imaging devices, a HPGe gamma spectrometer was used in order to obtain better quality gamma ray spectra for identification of the radionuclides present. The yellow 280 liter drum visible in Figure 8 contains a 200 liter drum, which in turn contains a 100 liter drum. The 100 liter drum contains the waste and the void between the 100 liter and the 200 liter drum is filled with concrete, about 5 cm thick. There is an air gap of a few centimeters between the outer 280 liter drum and the 200 liter drum. Real waste drums containing contamination and possibly activated waste were used.

At TSL, measurements were performed of both fixed objects and previously removed objects, now in storage. Given the nature and history of the accelerator facility, the main radionuclides observed are <sup>22</sup>Na, mainly originating from activated aluminum, and <sup>60</sup>Co, mainly originating from activated copper.



**Figure 8:** Measurement setup at Svafo, with the HPGe gamma spectrometer (1), H420 gamma camera (2) and GeGI gamma camera (3) observing a 280 liter waste drum.

### 4.3. Results

A few exemplary results of comparing Compton images obtained with the H420 and GeGI devices are shown in Figure 9 and Figure 10.

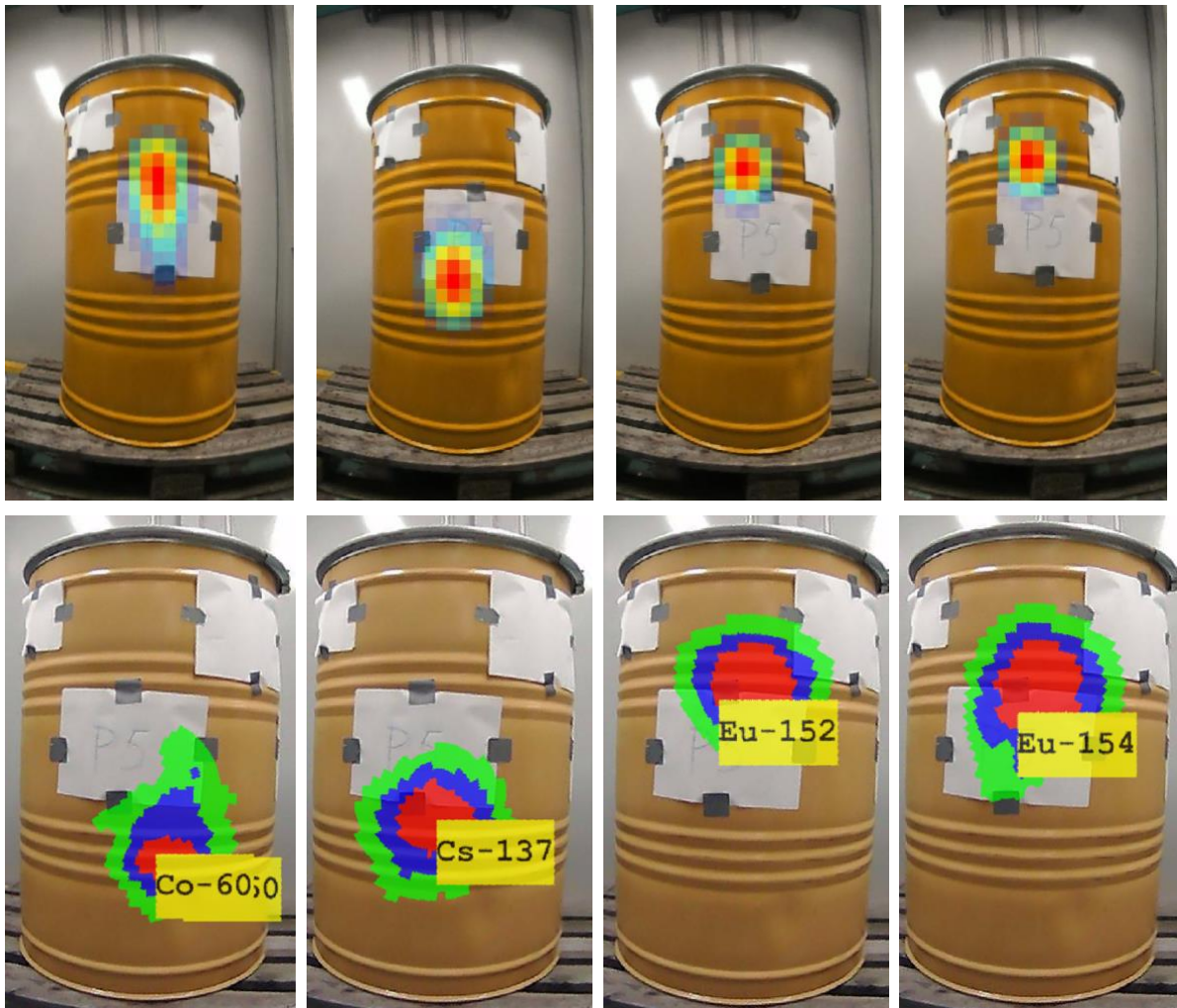


**Figure 9.** Compton imaging of a waste drum containing  $^{60}\text{Co}$ ,  $^{137}\text{Cs}$ ,  $^{152}\text{Eu}$  and  $^{154}\text{Eu}$  activities. Top row: H420 device in "high-resolution evaluation" mode. Bottom row: GeGI device. From left to right, gamma ray peaks of  $^{60}\text{Co}$ ,  $^{137}\text{Cs}$ ,  $^{152}\text{Eu}$  and  $^{154}\text{Eu}$  were selected.

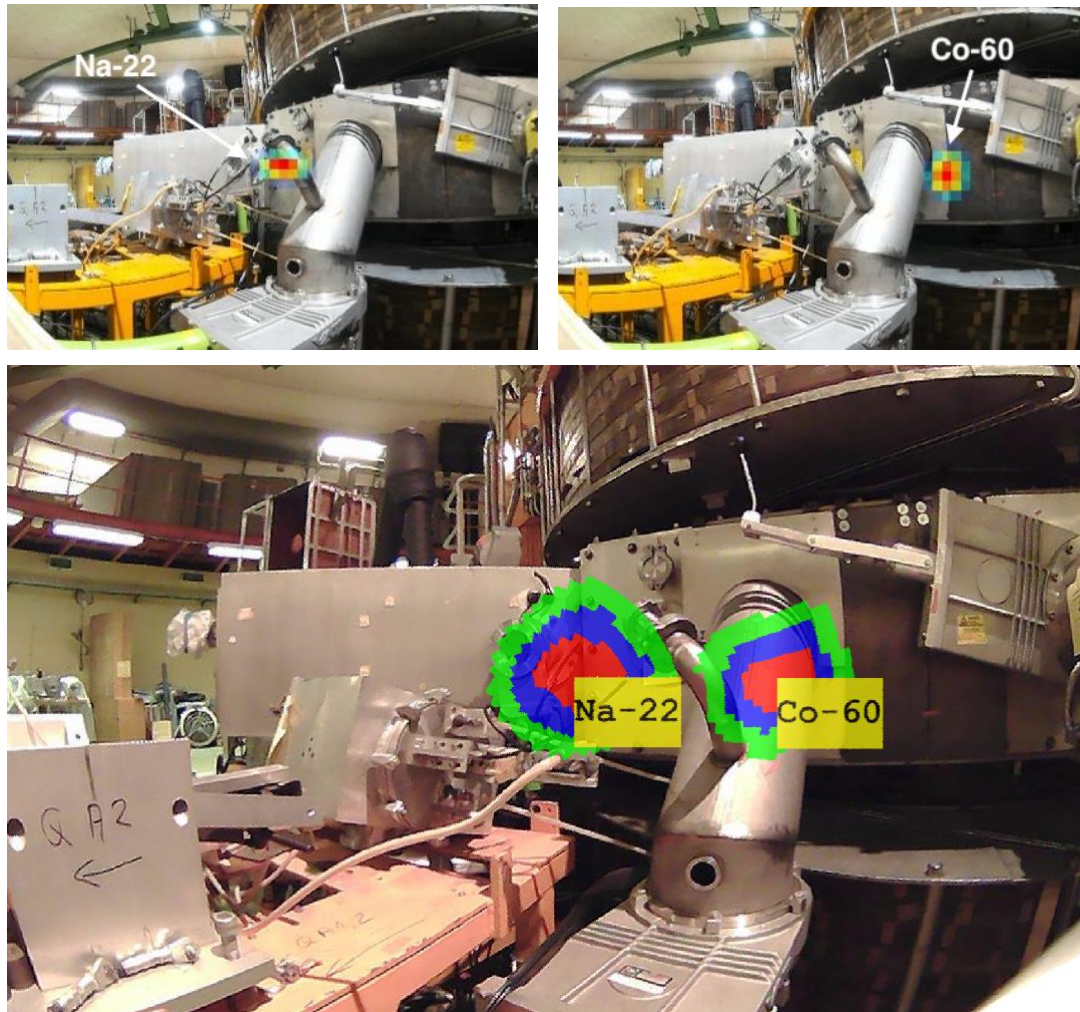


**Figure 10.** Compton imaging in the accelerator hall of the The Svedberg Laboratory. The top left and right show the  $^{22}\text{Na}$  and  $^{60}\text{Co}$  images with the H420 device in "high-resolution evaluation" mode. The bottom picture shows the GeGI combined image of these two radionuclides.

The results from the two imagers generally matched well. An exception, for unknown reason so far, are the  $^{60}\text{Co}$  images in Figure 9. The GeGI device was better at detecting low activities, partly because of a larger crystal surface area ( $64\text{ cm}^2$  vs.  $19\text{ cm}^2$ ) and partly because of the better energy resolution ( $0.3\%$  vs.  $1.1\%$  at  $662\text{ keV}$ ). The H420 was experienced to be easier to handle, partly because there is no detector cryogenic cooling system (the H420 is about half the volume and weight of the GeGI) and partly because of easier to use software. The difference in software capabilities might be because the H420 tested was a more recent version, purchased in 2021, compared to the GeGI which was purchased in 2017.

## **5. Conclusions**

The POSEIDON project activities between March 2024 and February 2025 have progressed along several lines, increasing knowledge and expertise in the Northern Countries. Monte Carlo simulations show the clear advantage of large CZT detectors compared to the presently used small detectors for PGET of spent nuclear fuel was demonstrated, justifying the further development of the large CZT detectors. The results of a first measurement campaign combining a tomographic setup at Uppsala University with a detector from IDEAS in Oslo and a collimator from HIP in Helsinki demonstrates the feasibility of PGET measurements using state-of-the-art large position-sensitive CZT detectors, showing that such detectors are a viable choice for future development of the PGET method. This experimental work is being complemented with Monte Carlo simulation of PGET of real spent nuclear fuel. First results, using a somewhat simplified gamma ray emission source, demonstrate that the Monte Carlo framework performs well. A measurement campaign using two commercial gamma ray imagers, the CZT-based H420 and the germanium-based GeGI, in a realistic nuclear waste setup at Svafo and a real-life decommissioning situation at TSL, has resulted in valuable practical experience with both imagers. The conclusion is that both imagers perform similarly, with the H420 being somewhat easier to handle and operate.

The POSEIDON activities are being continued for another year. Tomographic measurements at Uppsala will aim at a more fundamental understanding of the PGET method by investigating specific aspects that cannot be experimentally studied using real spent fuel. Improved Monte Carlo simulations of PGET using large position-sensitive CZT detectors will be performed, and the results combined with state-of-the-art image reconstruction. This will translate the experimental results to a real-life spent fuel situation. Gamma ray imaging experiments of objects related to decommissioning and legacy waste will focus on the detection of small amounts of fissile material and hazardous stable elements by active neutron interrogation.

### **Acknowledgements**

NKS conveys its gratitude to all organizations and persons who by means of financial support or contributions in kind have made the work presented in this report possible.

This work was supported by the Research Council of Finland (Flagship of Advanced Mathematics for Sensing Imaging and Modelling grant 359182).

### **Disclaimer**

The views expressed in this document remain the responsibility of the author(s) and do not necessarily reflect those of NKS. In particular, neither NKS nor any other organisation or body supporting NKS activities can be held responsible for the material presented in this report.

## 6. References

- Allison, J, Amako, K, Apostolakis, J, Arce, P, Asai, M, Aso, T, Bagli, E, Bagulya, A, Banerjee, S, Barrand, G, Beck, BR, Bogdanov, AG, Brandt, D, Brown, JMC, Burkhardt, H, Canal, P, Cano-Ott, D, Chauvie, S, Cho, K, Cirrone, GAP, Cooperman, G, Cortés-Giraldo, MA, Cosmo, G, Cuttone, G, Depaola, G, Desorgher, L, Dong, X, Dotti, A, Elvira, VD, Folger, G, Francis, Z, Galoyan, A, Garnier, L, Gayer, M, Genser, KL, Grichine, VM, Guatelli, S, Guèye, P, Gumplinger, P, Howard, AS, Hřivnáčová, I, Hwang, S, Incerti, S, Ivanchenko, A, Ivanchenko, VN, Jones, FW, Jun, SY, Kaitaniemi, P, Karakatsanis, N, Karamitros, M, Kelsey, M, Kimura, A, Koi, T, Kurashige, H, Lechner, A, Lee, SB, Longo, F, Maire, M, Mancusi, D, Mantero, A, Mendoza, E, Morgan, B, Murakami, K, Nikitina, T, Pandola, L, Paprocki, P, Perl, J, Petrović, I, Pia, MG, Pokorski, W, Quesada, JM, Raine, M, Reis, MA, Ribon, A, RistićFira, A, Romano, F, Russo, G, Santin, G, Sasaki, T, Sawkey, D, Shin, JI, Strakovsky, II, Taborda, A, Tanaka, S, Tomé, B, Toshito, T, Tran, HN, Truscott, PR, Urban, L, Uzhinsky, V, Verbeke, JM, Verderi, M, Wendt, BL, Wenzel, H, Wright, DH, Wright, DM, Yamashita, T, Yarba, J & Yoshida, H. 2016. Recent developments in GEANT4. Nucl Instrum Meth Phys Res A. 835: 186-225.
- Backholm, R, Bubba, TA, Bélanger-Champagne, C, Helin, T, Dendooven, P & Siltanen, S. 2020. Simultaneous reconstruction of emission and attenuation in passive gamma emission tomography of spent nuclear fuel. Inverse Problems & Imaging. 14: 317-337.
- Jansson, P, Jacobsson Svärd, S, Grape, S & Håkansson, A. 2013. A laboratory device for developing analysis tools and methods for gamma emission tomography of nuclear fuel. ESARDA Symposium 2013 - 35<sup>th</sup> Annual Meeting, JRC Technical Report <https://publications.jrc.ec.europa.eu/repository/bitstream/JRC83924/lcna26127enn.pdf>
- Laassiri, M, Rathore, V, Kalliokoski, M, Andersson, P, Dendooven, P. 2023. Position-sensitive detectors for nuclear fuel imaging (POSEIDON). NKS-473 [https://www.nks.org/en/nks\\_reports/view\\_document.htm?id=111010214698411](https://www.nks.org/en/nks_reports/view_document.htm?id=111010214698411)
- Mayorov, M, White, T, Lebrun, A, Brutscher, J, Keubler, J, Birnbaum, A, Ivanov, V, Honkamaa, T, Peura, P & Dahlberg, J. 2017. Gamma Emission Tomography for the Inspection of Spent Nuclear Fuel. 2017 IEEE Nuclear Science Symposium and Medical Imaging Conference (NSS/MIC), Atlanta, GA, USA.
- Saariokari, S, Dendooven, P, Laassiri, M & Brücken, JE. 2025. Nuclear fuel imaging using position-sensitive detectors. J Instrum. 20: C03012.
- Virta, R, Backholm, R, Bubba, TA, Helin, T, Moring, M, Siltanen, S, Dendooven, P & Honkamaa, T. 2020. Fuel rod classification from Passive Gamma Emission Tomography (PGET) of spent nuclear fuel assemblies. ESARDA Bulletin. 61: 10-21.
- Virta, R, Bubba, TA, Moring, M, Siltanen, S, Honkamaa, T & Dendooven, P. 2022. Improved Passive Gamma Emission Tomography image quality in the central region of spent nuclear fuel. Sci Rep. 12: 12473.



Title	Position-sensitive detectors for gamma ray imaging
Author(s)	Peter Dendooven <sup>1</sup> Santeri Saariokari <sup>1</sup> Peter Andersson <sup>2</sup> Sofia Godø <sup>3</sup> Anders Puranen <sup>4</sup> Gustav Pettersson <sup>4</sup> Stefan Jarl Holm <sup>2</sup> Erik Brücken <sup>1</sup> Mihaela Bezak <sup>1</sup> Matti Kalliokoski <sup>1</sup> Vikram Rathore <sup>2</sup> Mounia Laassiri <sup>5</sup> Ramsey Al Jebali <sup>3</sup> Aage Kalsæg <sup>3</sup>
Affiliation(s)	<sup>1</sup> Helsinki Institute of Physics, University of Helsinki, Helsinki, Finland <sup>2</sup> Department of Physics and Astronomy, Uppsala University, Uppsala, Sweden <sup>3</sup> Integrated Detector Electronics AS (IDEAS), Oslo, Norway <sup>4</sup> AB Svafo, Nyköping, Sweden <sup>5</sup> Department of Physics, Brookhaven National Laboratory, Upton, NY, USA
ISBN	978-87-7893-597-7
Date	April 2025
Project	NKS-R / POSEIDON (NKS_R_2022_136)
No. of pages	16
No. of tables	2
No. of illustrations	10
No. of references	8
Abstract max. 2000 characters	The POSEIDON project activities between March 2024 and February 2025 are summarized. Monte Carlo simulations show the clear advantage of large CZT detectors compared to the presently used small detectors for PGET of spent nuclear fuel was demonstrated: the efficiency to detect the full energy of the gamma rays from the decay of <sup>137</sup> Cs is more than 20 times larger. This justifies the further development of the large CZT detectors. The results of a first measurement campaign combining a tomographic setup at Uppsala University with a detector from IDEAS in Oslo and a collimator from

HIP in Helsinki demonstrates the feasibility of PGET measurements using state-of-the-art large position-sensitive CZT detectors, showing that such detectors are a viable choice for future development of the PGET method. This experimental work is being complemented with Monte Carlo simulation of PGET of real spent nuclear fuel. First results, using a somewhat simplified gamma ray emission source, demonstrate that the Monte Carlo framework performs well. A measurement campaign using two commercial gamma ray imagers, the CZT-based H420 and the germanium-based GeGI, in a realistic nuclear waste setup at Svafo and a real-life decommissioning situation at TSL, has resulted in valuable practical experience with both imagers. The conclusion is that both imagers perform similarly, with the H420 being somewhat easier to handle and operate. The activities have increased knowledge and expertise in the Northern Countries on several topics related to gamma ray imaging. A brief outlook of the continuing activities over the next year is presented.

Key words

gamma ray imaging, position sensitive detectors, semiconductor detectors, spent nuclear fuel, decommissioning, nuclear waste, tomography